SIMULATIONS OF CONDUCTION IN UNIFORM MYELINATED FIBERS

RELATIVE SENSITIVITY TO CHANGES IN NODAL AND INTERNODAL PARAMETERS

JOHN W. MOORE, RONALD W. JOYNER, MICHAEL H. BRILL, STEPHEN D. WAXMAN, AND MANUEL NAJAR-JOA

From the Department of Physiology, Duke University Medical Center, Durham, North Carolina 27710, Massachusetts Institute of Technology, Cambridge, Massachusetts 02139, and Harvard Medical School, Boston, Massachusetts 02115 U. S. A.

ABSTRACT Conduction of impulses in myelinated axons has been studied by a new method of computer simulation. The contributions of nodal and internodal characteristics and parameters were examined. Surprisingly, the conduction velocity, θ, was found to be quite insensitive to the nodal area or the exact description of its excitable processes. The conduction velocity also is relatively insensitive to the internodal length but much more sensitive to the myelin capacitance and axoplasm conductance. Qualitative change in θ with temperature depended on which temperature-sensitive parameters were included in the simulation.

INTRODUCTION

The first comprehensive analysis and theory of propagation of impulses in myelinated nerve fibers was developed by Rushton (1951). Subsequently, simulations for propagation of impulses in myelinated fibers have been carried out by a number of investigators, as indicated in Table I. As this table shows, a wide range of values have been used for the nodal membrane capacity, along with several descriptions for ionic conductances. The computations were carried out with different temperatures and different numerical integration methods. Although the simulations were done at several different temperatures, one might hope to be able to compare the different velocities thereby obtained. However, there are conflicting results of simulations, one showing linear (Hutchinson et al., 1970) and one reporting exponential (Hardy, 1973) dependences of the velocity on temperature. Some values of the simulated impulse velocity agree with experimental values while others disagree by a factor as large as two. For example, Hardy's (1973) standard data set gave a velocity of about one-half the experimental value. To achieve a velocity in reasonable agreement with the experimental

---

Dr. Najar-Joa's present address is: Departmento de Fisiologia, Facultad de Medicina, Universidad Nacional, Ciudad Universitaria, Mexico, 20, DF.

TABLE I

SIMULATION OF IMPULSE PROPAGATION IN MYELINATED FIBERS

Author	Year	Description of node kinetics	Nodal capacitance	Numerical integration method	Segments per internode	Δt	Temp	Velocity
			pF			μs	°C	m/s
FitzHugh	1962	Hodgkin-Huxley (6.3°C)	1.5	Explicit	8	0.75	6.3	11.9
Goldman and Albus (GA)	1968	Frankenhaeuser-Huxley (20°C)	1.65	Explicit "similar to FitzHugh"	10	0.05–0.15	20	18.5*
Hutchinson et al.	1970	Frankenhaeuser-Huxley		Explicit	5	7.5	20	19.2*
Koles and Rasminsky	1972	Frankenhaeuser-Huxley		Explicit	10	Adjusted	20	18.6
Hardy	1973	Hille (Dodge @22°C)	0.6–2.0	"Digital analog simulation"	5	0.2–0.4	15	9.5‡
Schauf and Davis	1974	Frankenhaeuser-Huxley		Explicit	10	Adjusted	10–50	18.8§
Dodge and this paper	1976	10-fold Hodgkin-Huxley	1.	Implicit‖	8	Adjusted	18.5	22.65

*Measured from published figures.

‡Standard data set.

§Measured from published figure at 20°C and extrapolated from 30 μm OD to 15 μm OD for comparison with others in table.

‖Cooley and Dodge (1966).

value, he made some drastic and some subtle changes (the validity for which he expresses some reservations) in the data set.

We had planned to initiate an extensive set of simulations to gain insight into the problems of impulse transmission in demyelinating diseases. When we noted all of the differences between different simulations as well as between experimental observations and simulations, we decided that it was first necessary to study systematically the problem of numerical simulation of impulse transmission. We hoped to gain insight into the sources of the differences cited above and to be able to synthesize a better model for the myelinated fiber.

As far as we could tell from the brief descriptions of the numerical methods, all of the published simulations used explicit integration methods. Previous evaluation of numerical integration methods for impulse generation and conduction in nonmyelinated fibers (Moore, Ramon, and Joyner [MRJ], 1975) had shown us that implicit numerical integration for partial differential equations was far superior to explicit methods. The latter were very prone to numerical instabilities, imposing strong restrictions on the size of the time step for a given increment in distance. The integration time steps used were quite small compared to those employed with explicit integration schemes for the squid axon (see Table I in MRJ, 1975). In the squid axon the speed of one process dominated all others; the time constant for turning on the sodium conductance at 6.3°C (e.g. Hodgkin-Huxley [HH] equations) is only about

one-fourth the next fastest process, the 1-ms time constant of the membrane. As the temperature is raised, the sodium turn-on rate increases and separates the time constants even further. In contrast, the membrane time constant for the node is usually taken as 25–27 μs, a fraction of the time constant for the sodium onset process even at 20°C (e.g. Frankenhaeuser and Huxley, 1964). Because the node has these two short time constants rather than a single dominant one, the integration problems for the myelinated fiber may be much more complex than for the squid axon.

The present studies of conduction in myelinated fibers were initiated with a hybrid integration method (implicit internode, explicit node) developed by one of us (M.B.). Immediately, however, it was found to be prone to instabilities also and to give an impulse velocity quite sensitive to the size of the time step and segment length. Therefore, we turned to a modification (by R.W.J.) of our Crank-Nicholson method of implicit solution of cable equations that we had used for nonmyelinated axons. This method turned out to be extremely accurate and fast; we could use large time steps without incurring problems of velocity errors or instability.

In summary, the intent of this first paper is to ascertain the bases of the differences in the simulation results to date, and to study the sensitivity of the velocity of propagation to integration methods as well as to changes in parameters including the description of the node itself. In the present report, we treat only uniform axons, i.e. ones in which all nodes and all internodes are identical. We consider only conduction velocity and not such issues as refractory period or the ability to carry high-frequency impulse trains.

METHODS

Previous publications have made only cursory reference to their numerical integration methods. We felt it useful to provide some detail about our implicit integration method that circumvents many of the problems of explicit methods. The Crank-Nicholson (CN) method of implicit solution of cable equations has been used to obtain solutions for propagating action potentials in uniform axons (MRJ, 1975) and in cells of variable geometry as shown in previous work by Ramon et al. (1975). The CN method has been demonstrated to be quite stable and relatively insensitive to variations in the size of integration step up to the point where oscillations occur in the falling phase of the action potential (presumably due to a mismatch in the size of the integration step and the time-course of the very fast transient peak in the sodium current, e.g. Moore and Ramón, 1974).

We have modified the general form of the Crank-Nicholson equations to include inhomogeneities in the specific membrane properties such as are found in nodal and nonnodal regions of a myelinated nerve. This provides a stable, fast, and accurate method to compute saltatory conduction of impulses in myelinated nerve fibers.

For the uniform nonmyelinated axon, the specific parameters of the membrane and the axoplasm are converted to equivalent units per length of fiber in the following way: $r_a(\Omega/\text{cm}) = R_a/\pi a^2$; $c_m(\text{F/cm}) = C_m \cdot 2\pi a$; and $g_m(\text{mho/cm}) = G_m \cdot 2\pi a$, where R_a is the specific axoplasm resistivity ($\Omega \cdot$ cm), C_m is the specific membrane capacitance (F/cm^2), and G_m (mho/cm^2) is the sum of the ionic conductances of the membrane model used ($G_{Na} + G_K + G_L$ in the Hodgkin-Huxley formulation). With these conventions, the general form of the CN equation for a homogeneous nonmyelinated fiber is:

$$a_j V_{j-1}^{t+1} + d_j V_j^{t+1} + b_j V_{j+1}^{t+1} = c_j,$$

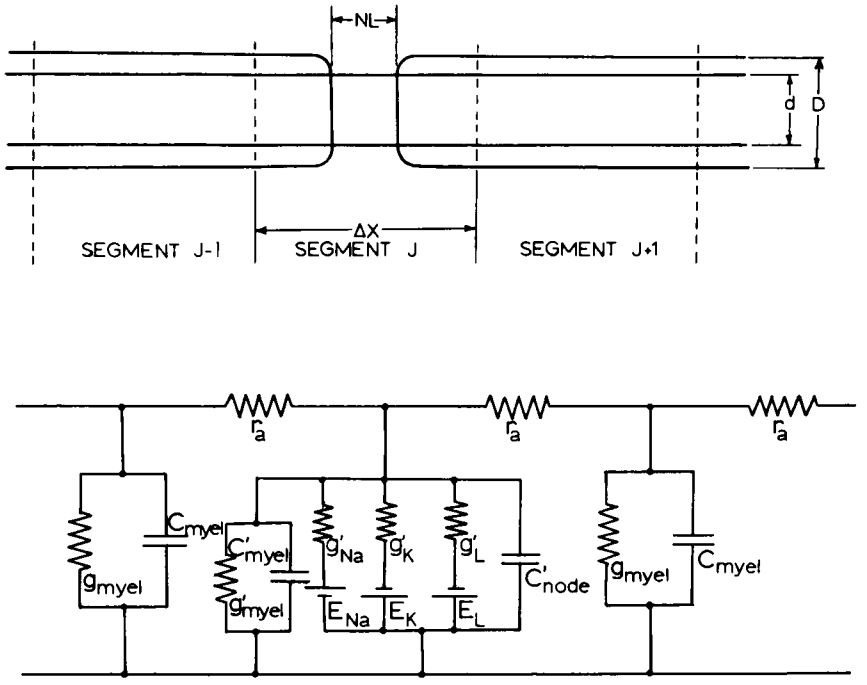

FIGURE 1 Schematic representation of the myelinated fiber to be modeled (above) and its electrical circuit equivalent (below).

for $a_j = -K, b_j = -K, d_j = 2(1 + K), c_j = 2(1 - K)V_j^t + K(V_{j-1}^t + V_{j+1}^t) - (2\Delta t/c_m)i_j^t$, $K = t/r_a c_m(\Delta x)^2$, where V_j^t is the potential of segment j at time t, and i_j^t is the ionic membrane current of segment j at time t. Since this equation is valid for each segment, we have, for an axon consisting of M segments, a set of M equations in M unknowns (the values of V_1^{t+1}, $V_2^{t+1}, \ldots V_M^{t+1}$), which can be solved simultaneously to advance the solution one time step for all the segments.

If we now represent a myelinated fiber as a series of isopotential segments of length Δx such that each node (node length = NL) is in the center of one of the segments, we can modify the parameters of the general equation to correspond to segments which contain a node or to segments which do not contain a node. This procedure is illustrated in Fig. 1. The top of the figure shows part of a myelinated fiber with the division into segments of length Δx shown. The bottom shows part of the equivalent cable circuit with the following conventions; (*a*) segments containing no node have a passive conductance and capacitance (g_{myel} and c_{myel}) in units of mho/cm and F/cm. (*b*) Segments containing a node have two parallel circuits representing the myelinated and unmyelinated parts of the segment. For the myelinated part of the segment we derive g'_{myel} and c'_{myel} from: $g'_{myel} = g_{myel}(\Delta x - NL)/\Delta x$ and $c'_{myel} = c_{myel}(\Delta x - NL)/\Delta x$. For the nodal part of the segment, we use

$$c'_{node} = C_{node} \cdot 2\pi a \cdot NL/\Delta x,$$

$$g'_{Na} = G_{Na} \cdot 2\pi a \cdot NL/\Delta x,$$

$$g'_K = G_K \cdot 2\pi a \cdot NL/\Delta x, \text{ and}$$

$$g'_L = G_L \cdot 2\pi a \cdot NL/\Delta x.$$

TABLE II

STANDARD PARAMETER SET

Temperature	18.5°C
Axon diameter (internal)	10 μm
Node area	100 μm^2
Node length	3.183 μm
Node capacitance	1 pF
Node description (HDHH)	Hodgkin-Huxley equations, with a high density of channels (10-fold)
	$\bar{g}_{Na}$ = 1,200 mmho/cm^2
	$\bar{g}_K$ = 360 mmho/cm^2
	$\bar{g}_L$ = 3 mmho/cm^2
Internode distance	2 mm
Myelin* thickness	2 μm
Myelin capacitance	0.005 μF/cm^2; 15.7 pF/cm
Myelin conductance	1.5 μmho/cm^2; 4.71 nmho/cm
Axoplasm resistivity	100 Ωcm; 127 MΩ/cm

*Myelin equated to 200 layers of cell membrane with a specific capacitance of 1 μF/cm^2 and leakage conductance of 0.3 mmho/cm^2.

Therefore, for each of the two types of segments we can now define the parameters of the general form of the CN equation. Case 1 (segments with no node): $K = \Delta t/r_a c_{myel}(\Delta x)^2$, and $i_j^t = V_j^t \cdot g_{myel}$. Case 2 (segments containing a node): $K = \Delta t/r_a c^*(\Delta x)^2$, where $c^* = c'_{myel} + c'_{node}$, and $i_j^t = V_j^t \cdot g'_{myel} + g'_{Na}(V_j^t - E_{Na}) + g'_K(V_j^t - E_K) + g'_L(V_j^t - E_L)$.

For tests of our integration method we used Dodge's parameter set as given in Table II. For comparison with others, we used the data set published in each paper. We used 10 segments to represent the internode except when investigating the sensitivity to these parameters.

RESULTS

Tests of Numerical Integration Method

For our primary reference point or "benchmark" problem, we chose to test our method with the results of Dodge (unpublished but graciously provided to us) because his integration method (iteration of solutions of simultaneous implicit equations, Cooley and Dodge, 1966) was known to be superior to the explicit integration methods used in the myelinated simulations published to date. Using Dodge's parameter set given in Table II, our numerical integration method gave precisely the same conduction velocity, 22.65 m/s, that he found.

The agreement between our computations and two secondary reference points was as good as could be expected. As secondary references we first used: the standard data set of Hardy (1973) and found a value of 8.9 m/s, close to his published value of 9.5 m/s but with smooth action potentials rather than his "clearly distorted" shapes. Then we used the data set of Goldman and Albus (1968), and found a value of 18.4 m/s and measured a velocity of 18.5 m/s from Fig. 3 in their paper.

We found (as have most workers) that, when a step of current is used for the stimulus, the shape of the action potential is distorted in the first few nodes. Termination of the axon at the far end also distorts the action potential at the last few nodes,

TABLE III

SENSITIVITY* OF CONDUCTION VELOCITY TO PARAMETERS

Parameters		Sensitivity
Internode structure		
Length		−0.05
Diameter: 200 layers myelin		+0.65
Number of layers proportional to diam. (constant cap/unit length)		+1.1
Axoplasm conductivity		+0.5
Turns of myelin (thickness)		+0.3
Myelin specific capacitance		−0.5
Myelin specific conductance		−0.01
Node structure and function		
Area		+0.07
Specific capacitance		−0.17
Leakage conductance		+0.02
Maximum specific conductivities		+0.18
Description at 20°C		
Frankenhaeuser-Huxley	24.5 m/s	
High-density Hodgkin-Huxley	24.1 m/s	

*Sensitivity defined as ratio of percentage change in θ to percentage change in parameters about the standard values given in Table II; domains shown in Fig. 2.

whether it be an open circuit or a short circuit. We used 10–20 nodes and averaged the conduction velocity over the central nodes, where it was quite uniform. We could have shaped the stimulus current to achieve a constant speed to the point of stimulation as we could for squid axon (Ramón et al., 1975). However, it did not seem to be worth the additional effort, because the simulations ran rapidly[1] with this numerical integration method.

Sensitivity to Parameters

All sensitivity studies were carried out with the reference standard parameters of Dodge given in Table II. The sensitivity of the conduction velocity to nodal and internodal characteristics are summarized in Table III and shown in Fig. 2.

INTEGRATION PARAMETERS One important factor in the speed of computation is related to the largest size of the time step which can be taken without causing serious errors or instability. We found that our numerical method could use time steps up to 12 μs with excellent stability; this is larger than step sizes used by most previous investigators (0.05–0.75 μs, see Table I). The amplitude of the action potential was insensitive to the integration time step, increasing only 0.2% (0.2 mV) when the step size was increased from 1 to 12 μs but the maximum rate of rise changed by 8.3% (from 828 to 904 V/s). We found a small linear increase in velocity with the time step up to 6 μs. The velocity error leveled off above a time step of 8 μs with a maximum value of 2.9% above that of an extrapolated zero time step. Considering that the uncertainty of

[1]The time to compute and plot for 2 ms of fiber time (with 10 μs time steps) over a 10-node fiber was only 3.5 min on the PDP15 (Digital Equipment Corp., Maynard, Mass.).

any and all the parameters is at best greater than this, it seems that a 10 μs time step is an optimum one to choose for speed and accuracy at 18.5°C. However for the remainder of these sensitivity studies, for greater accuracy, we used a 4-μs time step (sometimes even less for high temperatures).

We also found that the velocity of propagation was insensitive to the number of computational segments in the internode region. We normally used 10 internodal segments but for 5 internodal segments, found an identical velocity (within 0.03%). This was most reassuring because the velocity obtained in the original hybrid integration method was very sensitive to the number of internode segments.

NODE PARAMETERS The conduction velocity was found to be surprisingly insensitive to the specific nodal characteristic assignments. The velocity changes less than one fifth as rapidly as changes in the specific nodal capacitance and conductances; for example, changes as large as doubling the specific maximum voltage-sensitive conductances caused only an 11% increase in speed and for the specific capacitance only a 15% decrease.

The velocity was almost independent of the nodal area, a startling result. Previous analyses of scaling had paid careful attention to the nodal area; Goldman and Albus (1968) pointed out that Rushton's "corresponding states" required that the nodal length be constant (independent of the diameter). This totally unexpected insensitivity

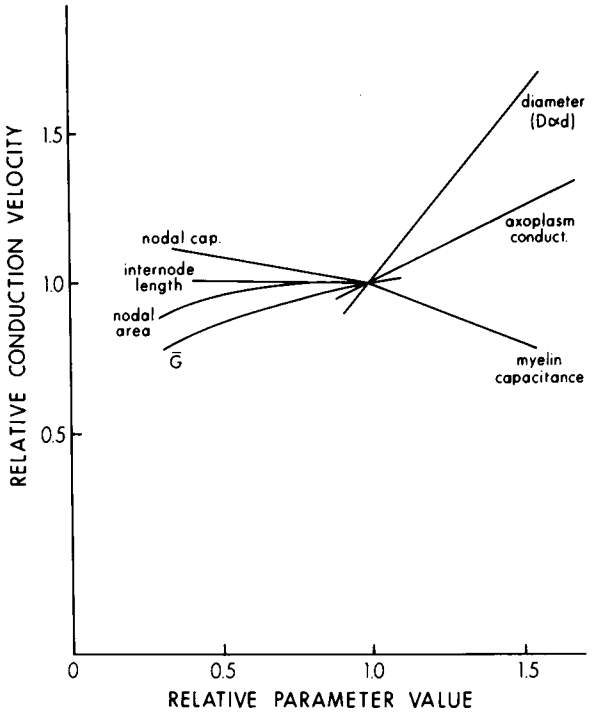

FIGURE 2 The relative sensitivity of the conduction velocity to nodal and internodal parameters. See Table III for numerical values.

to the nodal area may well be the result of the sum of nearly equal positive and negative sensitivities to capacitance and maximum number of sodium channels. Because the node is taken as a small isopotential patch, an increase in area would cause equal fractional increases in the nodal capacitance and maximum voltage sensitive conductances. Table III shows that these parameters affect the velocity in opposite and nearly equal ways.

To try to determine the sensitivity of the velocity of impulse propagation to the description of the nodal ionic conductances, we had to consider the following points:

Reference temperature. The Hodgkin-Huxley equations for the squid axon membrane are based on a standard temperature of 6.3°C. The standard temperature for the Frankenhaeuser-Huxley node model was 20°C and that for the Hille node model 22°C.

Q_{10} *of rate constants.* The squid axon rate constants have been found to have a Q_{10} of 3 by Hodgkin and Huxley (1952) and also by Moore (1958). For the node, Frankenhaeuser and Moore (1963) found essentially the same Q_{10} for the h and n processes but significantly lower values of Q_{10} for the m process (1.8 and 1.7 for α_m and β_m).

Reference values and Q_{10}*'s for conductance of axoplasm and ionic channels.* Our reference standard fiber from Dodge takes the axoplasm resistivity at 100 Ωcm at 18.5°C while Frankenhaeuser and Huxley (1964), dealing only with membrane action potentials, did not select a value. Axoplasm conductivity is important and we assign it a Q_{10} of 1.3, the usual value of electrolyte solutions. We have already noted the insensitivity of the conduction velocity to the maximum ionic conductances and expect that inclusion of a temperature coefficient of 1.4 (Moore, 1958) will make little difference. (The section on Temperature shows this to be the case.)

After consideration of these factors, we decided to make comparisons between the descriptions of the node at 20°C so as to introduce no change in the Frankenhaeuser-Huxley model, because our standard high-density HH (HDHH) model already had all rate constants multiplied by $3^{[18.5-6.3]/10}$ (= 3.82). We decided to extend the Q_{10} of 3 on the rate constants another 1.5°C. It seemed unnecessary to introduce temperature coefficients for the conductances already 10-fold higher than the HH values. To put the nodes in the same internodal setting we neglected the temperature sensitivity of the axoplasm resistivity and took it as 100 Ωcm at 20°C.

With these parameters we found a velocity of 24.1 m/s for our HDHH node and 24.5 m/s for a Frankenhaeuser-Huxley (FH) node. This remarkably small difference of only 1.6% may seem fortuitous but we must point out that we have a very limited freedom of choice here. If we had given the ionic conductances a Q_{10} of 1.4 referred to 6.3°C, the HDHH node would have given the fiber a 6% higher velocity than one with the FH node. But this increase could have been offset by assuming the smaller Q_{10}'s proposed by Frankenhaeuser and Moore for the sodium processes. One could run these simulations but we felt that they were pointless.

The essential and very important point that comes through is that the conduction velocity in a myelinated fiber is quite insensitive to the excitable nodal area or the exact method of description of its excitable processes. However, this does not hold for a demyelinating disease which exposes extra nonexcitable membrane at a node.

INTERNODE PARAMETERS The conduction velocity is almost independent of the length of the internode. In a companion paper (Brill et al., 1977) we have investigated conduction in our standard fiber when the internodal length is varied from 25 μm, where propagation characteristics approach the case of a continuous axon, to the maximum length which will sustain conduction, almost 10,000 μm. In agreement with Dodge (1978), we found a broad maximum in velocity between internode lengths of 1,000 and 2,000 μm. That is, the conduction velocity would be independent of the internode length from small changes around 1,500 μm.

The myelin sheath conductance has a negligible effect on the conduction velocity but an increase in the myelin specific capacitance causes a pronounced reduction in velocity. The original velocity can be restored by increasing the number of turns of myelin but a larger fractional change is required. The conduction velocity is moderately sensitive to the axoplasm conductivity and can be increased by more than half the increase in this parameter. A similar fractional increase in velocity can be obtained by an increase in the diameter, if the number of turns of myelin insulation is held constant. But enlarging the circumference of the myelin while holding its thickness fixed causes the capacitance per unit length to increase. If we increase the myelin thickness in proportion to the axon diameter (the proportionality found in peripheral fibers) we keep a constant capacitance per unit length and find the greatest fractional increase in velocity (slightly better than one for one).

We also looked for that distribution of myelin and axoplasm which would provide the maximum velocity in an axon with a fixed outside diameter. We found a maximum value for an inner-to-outer diameter ratio of 0.62, in good agreement with other values predicted (e.g. 0.6 Rushton, 1951; 0.7 Hodgkin, 1964), or simulated (Smith and Koles, 1970; Dodge, 1978) and with anatomical observations of 0.7 (from a careful literature search, L. Goldman, personal communication).

TEMPERATURE DEPENDENCE OF IMPULSE VELOCITY Because of the above noted ambiguities and uncertainties in how to estimate the effect of temperature on the parameters of myelinated nerve and because of the divergent velocity-temperature relations of different simulations, it seemed worthwhile to address the question of the contribution of the various temperature coefficients. A summary of the results is shown in Fig. 3.

Rate constants. We compared the functional relation between conduction velocity and temperature for the Frankenhaeuser-Moore Q_{10}'s and the standard Q_{10} of 3 for all rate constants of Hodgkin and Huxley normally used for squid axons. Both gave an essentially linear velocity vs. temperature relation up to about 30°C, beyond which the action potential amplitude begins to decline rapidly. The conduction velocity found for Q_{10}'s = 3 was: $\theta = (9 + 0.767 \cdot T)$ m/s,[2] for T in °C. This is remarkably and curiously close to the experimental observations of Hutchinson et al. (1970), for a 15 μm diameter fiber: $\theta = (9 + 0.9T)$m/s. Although their simulations also gave a linear relation, both the slope and intercept were more than double these experimental values.

[2]Over the limited range of 15°–25°C, this is straight enough on a semilog plot to extract a "Q_{10}" of 1.43.

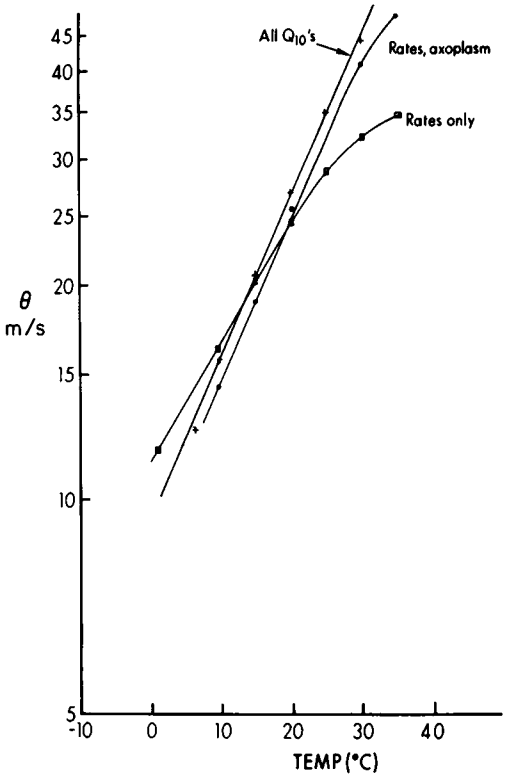

FIGURE 3 The relationship between conduction velocity and temperature depends on which parameters are given temperature coefficients. This figure shows the relationships for inclusion of membrane conductance rate constants only, rate constants plus axoplasm conductance, and these two plus maximum ionic conductances.

Axial resistivity and rates. Electrolytes show a temperature increase in conductance with a Q_{10} of 1.25 to 1.3. Axoplasm conductivity is electrolytic and should be given a similar temperature dependence. When the axial conductivity of standard fiber was assigned a Q_{10} of 1.3, (along with a Q_{10} of 3 for the rates) the velocity became an exponential function of the temperature from 10 to 30°C with a Q_{10} of 1.68. The inclusion of the temperature sensitivity of the axial resistance is sufficient to change a linear relation to an exponential and to be the probable resolution of these differences in the functional relationship found by the previous workers.

Maximum conductances. Moore (1958) reported a temperature coefficient of 4%/°C for the maximum ionic conductances in squid axon. This is frequently included in simulations for these axons as a Q_{10} of 1.4 or 1.5. When this is included (along with those above), it increases the velocity by a small fraction (0.18, Table III) of the increase in the conductances but does not change the functional relationship from exponential and does not make any apparent change in the Q_{10}.

DISCUSSION

The several questions which led to this inquiry have been satisfactorily answered or given a basis of understanding.

One of the most interesting revelations of this investigation is that the internodal structure and parameters have far more control of the conduction velocity than does the node. This is important in understanding the contribution of design factors and in normal and pathological conditions. In biological terms, it lends significance to the observation that internodal distances, rather than nodal geometry, are modified (compared to normal peripheral or white matter fibers) in those central axons which function as delay lines (Waxman, 1975; Waxman and Melker, 1971; Meszler et al., 1974). Furthermore it points out which simulation parameters (and measurements) are crucial and which do not need as accurate a specification.

It is reassuring that the choice of the exact and precise description for the excitable membrane is not as important as getting the approximately correct time constants and amplitudes of the conductances.[3] We thus learn that one need not be concerned about whether the description is absolutely correct in terms of permeabilities or conductances. Nor do we have to include such subtleties as the small shifts in rate constants that Hardy considered. Dr. Frederick A. Dodge told us that his studies showed that the correct threshold level was the most important characteristic of the nodal membrane description.

These insights may help to place previous results of simulations in context. For example, FitzHugh chose a nodal "area" of 3,000 μm^2 to get sufficient resting conductance from the HH equations to match an experimental measurement of the nodal resistance. Our reference node uses a 10-fold increase in the HH channel density for a 100 μm^2 node. Thus FitzHugh's node is equivalent to our 100 μm^2, along with another threefold increase in the number of channels and a 50% increase in the node capacitance. The sensitivity to these factors is equal and opposite (Table III), so that his conduction velocity should be close to what we predict at his temperature choice of 6.3°C. Using a Q_{10} of 1.3 for the axial resistance brings us into close agreement for this factor and we find a velocity of 12.5 m/s compared to his 11.9 m/s.

These simulations also reveal another example of the elegance of the design of the myelinated fibers: the insensitivity of conduction to nodal constrictions. Anatomical studies of myelinated fibers frequently show a "strangulation" or reduction in diameter at nodes. The amount of strangulation is not constant but varies with the diameter. In his analytical paper Dun (1970) first raised the question as to how this might affect conduction velocities. Although he goes to great pains to calculate the diameter and length of nodes as a function of fiber diameter, FitzHugh (1973) pointed out an error in his logic, and the present investigation shows that nodal size is not an important vari-

[3]This insensitivity to conductances is reminiscent of the insensitivity of the squid axon membrane action potential shape to the number of ionic channels (e.g., Moore and Ramón, 1974).

able. Our simulations show that a strangulation resulting in one-half the normal nodal area reduces the conduction velocity by only 3.8%! For greater internodal lengths, the percentage effect is even smaller. Such differences should not be experimentally detectable because they are less than the accuracy of most determinations of fiber diameter and velocity.

Our simulations resolve the differences in the simulation literature as to the functional relation of the conduction velocity to temperature. The relation is linear if the rate constant temperature sensitivities alone are considered; when the variation of axoplasm conductivity is included, it becomes exponential, implying a Q_{10}. However the Q_{10} is so small that measurements must be made over a wide temperature range to distinguish the exponential from a linear relation.

It seems reasonable and necessary to include the thermal coefficient of the axoplasm in simulations to match the real world and leads one to expect an exponential relation with temperature. However, most experimental studies of velocity of conduction in myelinated fibers report a linear relation with temperature (Frankenhaeuser and Waltman, 1959; Hutchinson et al., 1970; Paintal, 1965). Although Hardy reports an exponential relation over only a 3°C range in temperature, this is hardly sufficient to establish the point, especially for the degree of data scatter. The resolution of this small inconsistency awaits further experimentation.

We are very grateful to Dr. Frederick Dodge for providing us with his unpublished model fiber and node description. We had originally planned to adapt the widely used HH equations to fit the best voltage clamp data on myelinated fibers, thinking that this might become the model of choice. However, after noting the insensitivity of conduction velocity to the nodal descriptions or maximum conductances, we think that this is not important. Dodge's use of the HH equations with all $\bar{g}$'s increased 10-fold is simpler than our choices and gives approximately the same velocity. While HDHH equations provide a simple and convenient reference standard for myelinated axon velocity calculations, it may be that they will give different results for refractoriness and drug action from equations developed from voltage clamp measurements on nodes.

We expect our observations on parameter sensitivities to apply to mammalian nerves even though the simulations are based on descriptions of squid axons or amphibian myelinated nerve at temperatures lower than 25°C. Nevertheless, these descriptions have been extrapolated to higher temperatures by scaling rate constants with a Q_{10} (from measurements in the amphibian fibers) and impulse conduction occurred up to a temperature of 50°C (Schauf and Davis, 1974). Curiously, although both the squid axon and its description by Hodgkin and Huxley fail to propagate above about 30°C (Huxley, 1959), when the HH equations are used to describe a node, simulated impulses can propagate in the myelinated fiber up to above 40°C. Therefore we feel that, when data on mammalian nodes are available and put into appropriate internodal structures and simulations are run with schemes similar to ours, the major observations associated will be similar to what we have reported.

We appreciate the generosity of Dr. Frederick A. Dodge for sharing with us his model and unpublished simulations and are further grateful for his careful reading of the manuscript. We appreciate helpful comments from Doctors Bertil Hille, Larry Goldman, Robert Stämpfli, and Richard FitzHugh.

This work was supported by National Institutes of Health grants NS03437, NS12307, K04-00010, and TO 1-Ey00090 and the Health Sciences Fund.

Received for publication 3 November 1977.

REFERENCES

BRILL, M. H., S. G. WAXMAN, J. W. MOORE, and R. W. JOYNER. 1977. Conduction velocity and spike configuration in myelinated fibers. Computed dependence on internode distance. *J. Neurol. Neurosurg. Psychiatry.* **40**:769–774.

COOLEY, J. W., and F. A. DODGE. 1966. Digital computer solutions for excitation and propagation of the nerve impulse. *Biophys. J.* **6**:583.

DODGE, F. A. 1978. Impulse propagation in myelinated nerve fiber. *Biophys. J.* In press.

DUN, F. T. 1970. Length and diameter of the node of Ranvier. *IEEE (Inst. Electr. Electron. Eng.)* Trans. *Biomed. Eng.* **17**:21.

FITZHUGH, R. 1962. Computation of impulse initiation and saltatory conduction in a myelinated nerve fiber. *Biophys. J.* **2**:11–21.

FITZHUGH, R. 1973. Dimensional analysis of nerve models. *J. Theor. Biol.* **40**:517.

FRANKENHAEUSER, B., and A. F. HUXLEY. 1964. The action potential in the myelinated nerve fibre of Xenopus laevis as computed on the basis of voltage clamp data. *J. Physiol. (Lond.).* **171**:302–325.

FRANKENHAEUSER, B., and L. E. MOORE. 1963. The specificity of the initial current in myelinated nerve fibres of Xenopus laevis. Voltage clamp experiments. *J. Physiol. (Lond.).* **169**:438.

FRANKENHAEUSER, B., and B. WALTMAN. 1969. Membrane resistance and conduction velocity of large myelinated nerve fibres from *Xenopus laevis*. *J. Physiol. (Lond.).* **148**:677.

GOLDMAN, L., and J. S. ALBUS. 1968. Computation of impulse conduction in myelinated fibers. Theoretical basis of the velocity-diameter relation. *Biophys. J.* **8**:596–607.

HARDY, W. L. 1973. Propagation speed in myelinated nerve. I. Experimental dependence on external Na^+ and on temperature. *Biophys. J.* **13**:1054–1070.

HARDY, W. L. 1973. Propagation speed in myelinated nerve. II. Theoretical dependence on external Na^+ and on temperature. *Biophys. J.* **13**:1071–1089.

HODGKIN, A. L. 1964. The Conduction of the Nervous Impulse. Liverpool University Press, Liverpool, U.K.

HODGKIN, A. L., and A. F. HUXLEY. 1952. A quantitative description of membrane current and its application to conduction and excitation in nerve. *J. Physiol. (Lond.).* **117**:500.

HUTCHINSON, N. A., Z. J. KOLES, and R. S. SMITH. 1970. Conduction velocity in myelinated nerve fibres of Xenopus laevis. J. Physiol. **208**:279–289.

HUXLEY, A. F. 1959. Ion movements during nerve activity. *Ann. N. Y. Acad. Sci.* **81**:221.

KOLES, Z. J., and M. RASMINSKY. 1972. A computer simulation of conduction in demyelinated nerve fibres. *J. Physiol. (Lond.).* **227**:351–364.

MESZLER, R. M., G. D. PAPPAS, and M. V. L. BENNETT. 1974. Morphology of the electromotor system in the spinal cord of the electric eel, *Electrophorus electricus*. *J. Neurocytol.* **3**:251.

MOORE, J. W. 1958. Temperature and drug effects on iquid axon membrane ion conductances. *Fed. Proc.* **17**:447. (Abstr.).

MOORE, J. W., and F. RAMÓN. 1974. On numerical integration of the Hodgkin and Huxley equations for a membrane action potential. *J. Theor. Biol.* **45**:249.

MOORE, J. W., F. RAMÓN, and R. W. JOYNER. 1975. Axon voltage-clamp simulations. I. Methods and tests. *Biophys. J.* **15**:11.

PAINTAL, A. S. 1965. Effects of temperature on conduction in single vagal and saphenous myelinated nerve fibres of the cat. *J. Physiol. (Lond.).* **180**:20.

RAMÓN, F., R. W. JOYNER, and J. W. MOORE. 1975. Propagation of action potentials in inhomogeneous axon regions *Fed. Proc.* **34**:1357.

RUSHTON, W. A. H. 1951. A theory of the effects of fiber size in medullated nerve. *J. Physiol. (Lond.).* **115:** 101.

SCHAUF, C. L., and F. A. DAVIS. 1974. Impulse conduction in multiple sclerosis: A theoretical basis for modification by temperature and pharmacological agents. *J. Neurol. Neurosurg. Psychiatry.* **37:**152–161.

SMITH, R. S., and Z. J. KOLES. 1970. Myelinated nerve fibers. Computed effect of myelin thickness on conduction velocity. *Am. J. Physiol.* **219:**1256.

WAXMAN, S. G. 1975. Integrative properties and design principles of axons. *Int. Rev. Neurobiol.* **18:**1.

WAXMAN, S. G., and R. J. MELKER. 1971. Closely spaced nodes of Ranvier in the mammalian brain. *Brain Res.* **32:**445.